

ULTRASONIC ATTENUATION RESULTS OF THERMOPLASTIC RESIN COMPOSITES UNDERGOING THERMAL AND FATIGUE LOADING

Eric I. Madaras
NASA Langley Research Center
MS 231
Hampton, VA 23681-0001

INTRODUCTION

Before airframe manufacturers introduce new materials into aeronautic structures, they require that these materials must be fully characterized for the environment they will be used in. For high speed aircraft, this would include the material's response to thermal and fatigue loading representative of high numbers of flight cycles. At the same time that these materials are undergoing the necessary mechanical testing, it is prudent to also investigate nondestructive evaluation (NDE) methods that can be used in the field to assess the condition of these new materials simultaneously with their mechanical evaluation.

As part of an effort to obtain the required information about new composites for aviation use, materials and NDE researchers at NASA are jointly performing mechanical and NDE measurements on new composite materials. The materials testing laboratory at NASA is equipped with environmental chambers mounted on load frames that can expose composite materials to thermal and loading cycles representative of flight protocols. Applying both temperature and load simultaneously will help to highlight temperature and load interactions during the aging of these composite materials.

This report highlights our initial ultrasonic attenuation results from thermoplastic composite samples that have undergone over 4000 flight cycles to date. Ultrasonic attenuation measurements are a standard method used to assess the effects of material

degradation [1]. Recently, researchers have shown that they could obtain adequate contrast in the evaluation of thermal degradation in thermoplastic composites by using frequencies of ultrasound on the order of 24 MHz [2]. In this study, we address the relationship of attenuation measured at lower frequencies in thermoplastic composites undergoing both thermal and mechanical loading. We also compare these thermoplastic results with some data from thermoset composites undergoing similar protocols. The composite's attenuation is reported as the slope of attenuation with respect to frequency, defined as $\beta = \Delta\alpha(f)/\Delta f$. The slope of attenuation is an attractive parameter since it is quantitative, yet does not require interface corrections like conventional quantitative attenuation measurements [3]. This latter feature is a consequence of the assumption that interface correction terms are frequency independent. Uncertainty in those correction terms can compromise the value of conventional quantitative attenuation data [3, 4]. Furthermore, the slope of the attenuation more directly utilizes the bandwidth information and in addition, the bandwidth can be adjusted in the post processing stage to compensate for the loss of dynamic range of the signal as the composites age.

EXPERIMENT

The samples used in this study are composites made from a high modulus fiber with a commercially available thermoplastic matrix. They are 16 ply thick, dog bone shaped panels which use a conventional ply lay-up and are manufactured by a major aeronautic company. Each sample is 122 cm long by 30.5 cm wide.

The environmental chambers can control temperature from -54°C to 344°C . They are also capable of applying loads ranging either from 0 to 22 or 50 kips. These chambers exposed the thermoplastic composite samples to thermal and load variations typical of supersonic flight. The temperatures used were below the thermoplastic's glass transition temperature. Samples were exposed to one of two load levels that emulated typical supersonic flight conditions. The lower loading condition was referred to as the low strain protocol and the higher loading condition that produced a 50 % greater strain was denoted as the high strain protocol.

It was preferred that the testing protocol would not be disrupted by removing the samples from the environmental chambers frequently. Thus, the measurements were made with an in-situ scanning system that was constructed to measure the composite samples at room temperature while they were mounted in the environmental chambers. This in-situ system constrained the scan regions to those areas of the composite samples that were exposed inside the chambers. The system used a 5 MHz, 5 cm focal length, 1.2 cm diameter immersion transducer. A water bubbler was used to couple the ultrasound to the samples. The length of the water path placed the composite material in the transducer's focal zone.

The ultrasonic system was microcomputer controlled to synchronize the measurements with sample location. A broad band, pulser-receiver computer card and a 100 MHz, 8 bit digitizing card were contained in the microcomputer. For this study, the system digitized at 25 MHz. The rf signals were captured and stored for post processing. The samples were scanned in raster format in 0.254 cm steps. Because of physical constraints within the environmental chambers, the samples had to be scanned in three overlapping scan regions of 25 cm by 25 cm areas. During subsequent processing, data sets or images from adjacent scanned regions were tiled together to produce a composite image with a nominal size of 60 cm by 25 cm.

The slope of attenuation with respect to frequency was determined from the measurements by first calculating the Fast Fourier Transform (FFT) power spectrum from front and first back wall echoes. Each echo that was transformed was centered in a digital gate using a 1.28 μ s long Hamming window. We used the first echo's FFT power spectrum, $S_f(f)$, to normalize the back wall echo's FFT power spectrum, $S_b(f)$. Finally, we convert the data to logarithmic form and normalize by thickness to obtain an apparent attenuation, $\alpha_a(f)$, which was not corrected for interface losses:

$$\alpha_a(f) = \ln [S_b(f) / S_f(f)] / 2t. \quad \text{Eq. 1}$$

This data was then fitted to a linear equation:

$$\alpha_a(f) = \beta * f + I, \quad \text{Eq. 2}$$

where β is the slope of the attenuation with respect to frequency and I is the function's intercept. Since the interface transmission and reflection coefficients are assumed to be frequency independent, they will in general be reflected in the intercept term, I , while β will represent the frequency dependent components of the materials. As can be seen by the rf traces in figures 1a and 1b, the frequency content of the echoes is being severely modified by the attenuation after 4048 flight cycles compared to signals from samples after only 310 flight cycles. To process the data consistently, the fit to the data was restricted to the frequency range of 1.56 to 5.47 MHz, frequencies for which there was adequate signal to noise ratio. The data was processed in this manner at each independent site.

RESULTS AND DISCUSSION

Typical slope of attenuation images of thermoplastic composites that have undergone different numbers of flight cycles under the low strain protocol are shown in figure 2. Figure

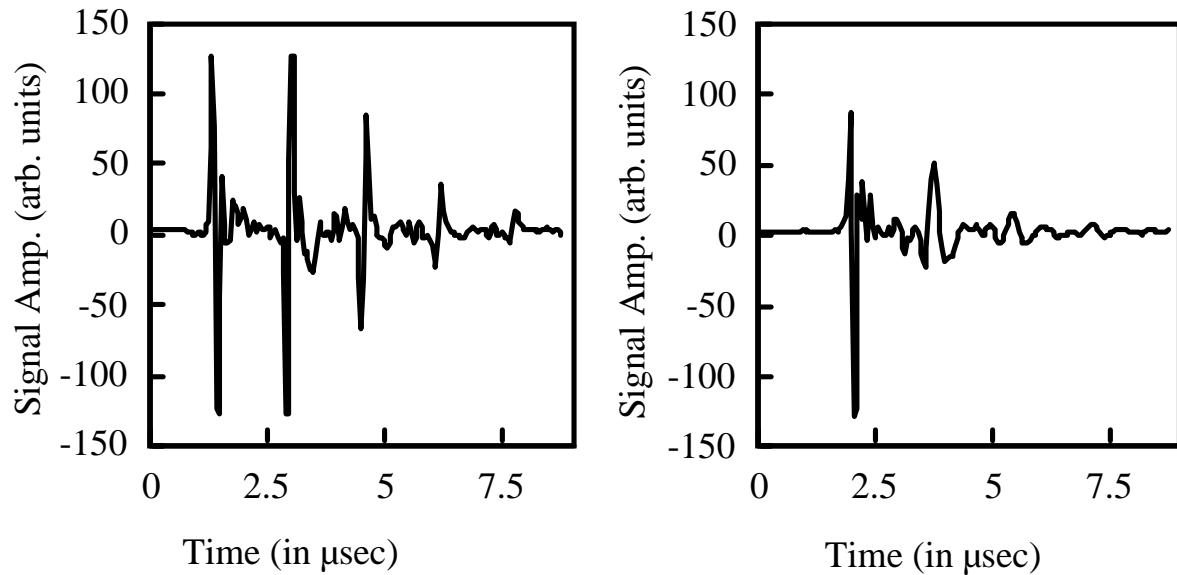


Figure 1. a) An rf trace from a sample that has undergone only 310 flight cycles. b) An rf trace from a sample that has undergone 4048 flight cycles. The horizontal axis is time and the vertical axis is signal amplitude.

2a shows a panel aged to 262 flight cycles. Figures 2b and 2c show a different panel aged to 1815 cycles and 3548 cycles respectively. The average attenuation and standard deviation increases from $0.798 \pm 0.537 \text{ cm}^{-1} \text{ MHz}^{-1}$ at 262 flight cycles to $1.42 \pm 0.46 \text{ cm}^{-1} \text{ MHz}^{-1}$ at 1815 flight cycles to $3.22 \pm 0.94 \text{ cm}^{-1} \text{ MHz}^{-1}$ at 3548 flight cycles. Several qualitative features are easily identified. First, the slope of attenuation increases progressively with the number of flight cycles. Second, as the samples are cycled, small islands of high β appear throughout the image, a few examples of which are circled in figures 2b and 2c. Comparison of figure 2b with figure 2c indicates that existing small islands of high β are increasing in size and in magnitude and additional islands of high β are appearing with increasing number of cycles.

Figure 3 shows slope of attenuation images of thermoplastic composites that have undergone various numbers of flight cycles under the high strain protocol. Figure 3a shows a panel aged to 310 flight cycles. Figures 3b and 3c show a different panel aged to 1868 cycles and 4048 cycles respectively. The average slope of attenuation and the standard deviation increased from $1.06 \pm 0.31 \text{ cm}^{-1} \text{ MHz}^{-1}$ after 310 flight cycles to $3.54 \pm .80 \text{ cm}^{-1} \text{ MHz}^{-1}$ after 1868 flight cycles to $4.36 \pm 1.05 \text{ cm}^{-1} \text{ MHz}^{-1}$ after 4048 flight cycles. As in figure 2, it can be seen that the slope of attenuation increases as the number of flight cycles increases. Also, even after a few hundred flight cycles at high strain, small islands of higher attenuation are appearing in the image, an example of which is a circled in figure 3a. By 4048 high strain flight cycles, the generally high attenuation makes identification of the local high β sites difficult to discern in the images.

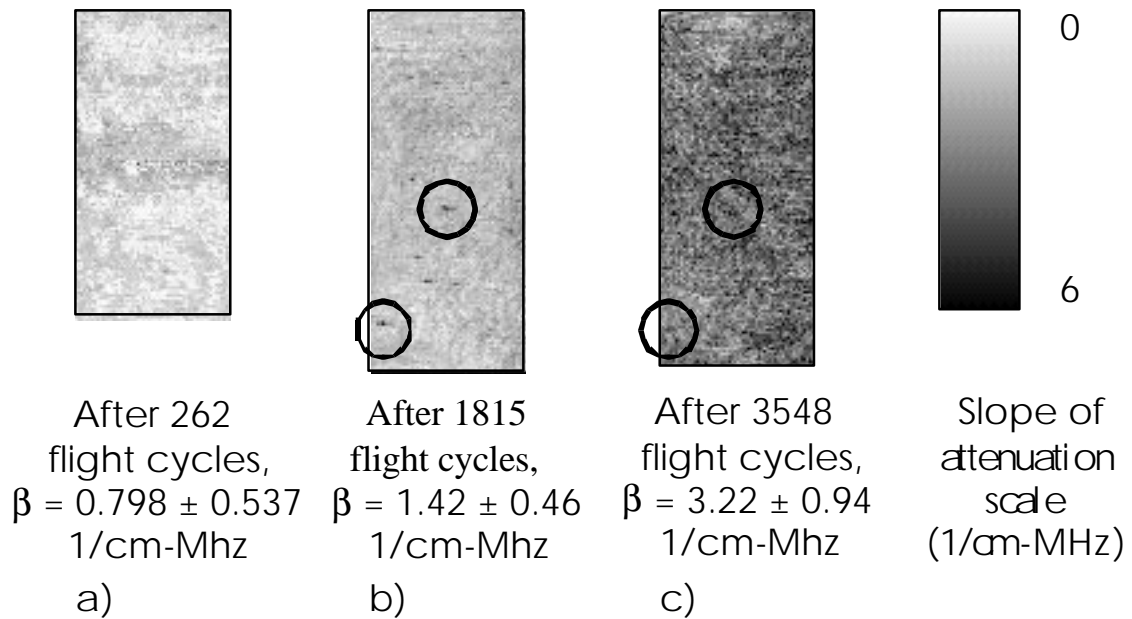


Figure 2. Three slope of attenuation images for thermoplastic composites that have undergone low strain flight cycles. A few examples of areas of high β are circled in figures 2b and 2c.

Comparison of figures 2 and 3, which are displayed on the same scale, shows the relative effects of strain on attenuation. The images of the thermoplastic composites show examples where a significantly accelerated growth in the slope of attenuation values accompany a 50% increase in strain. It appears that the samples undergoing the high strain protocol have almost doubled the slope of attenuation values compared to the low strain protocol panels.

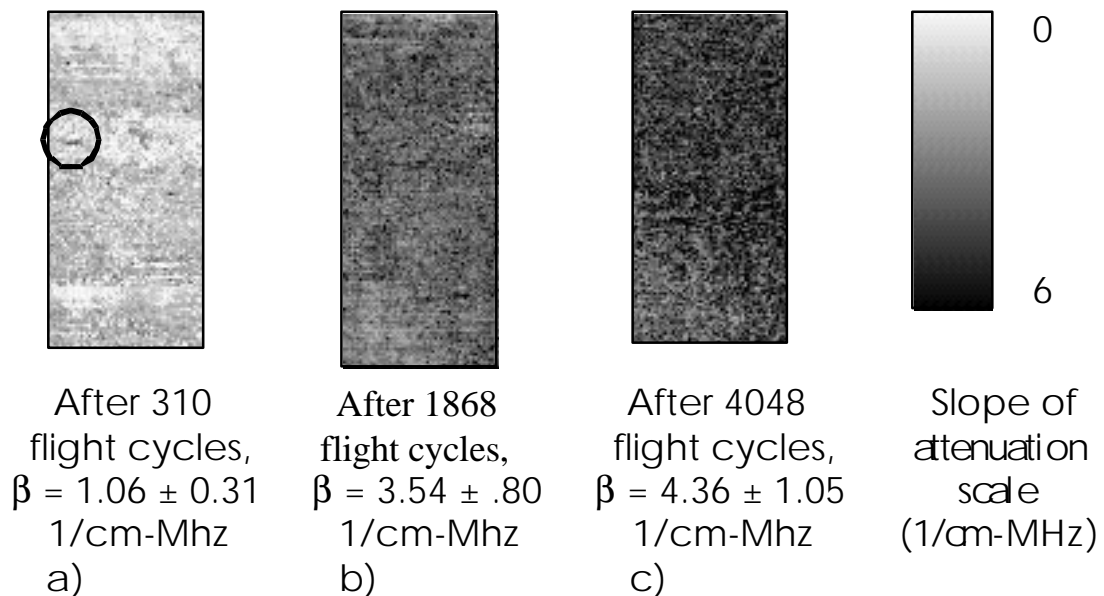


Figure 3. Three slope of attenuation images for thermoplastic composites that have undergone high strain flight cycles. . An example of an area of high β is circled in figures 2a.

Figure 4 shows a graph of the slope of attenuation versus the number of flight cycles for the thermoplastic high strain and low strain samples and for thermoset composites that also underwent similar high strain and low strain protocols. The thermal protocols for the thermoset and thermoplastic composites were different, being scaled by their respective manufacturer's suggested thermal limitations. The general trend of β as the number of flight cycles increases is seen for the thermoplastic composites that experienced either low strain or high strain protocols. The β for thermoplastic composite samples undergoing the high strain protocol ranges from near $1 \text{ cm}^{-1} \text{ MHz}^{-1}$ at low number of flight cycles up to $5 \text{ cm}^{-1} \text{ MHz}^{-1}$ at 4000 flight cycles. The β for thermoplastic composite samples undergoing the low strain protocol range from just below $1 \text{ cm}^{-1} \text{ MHz}^{-1}$ at low flight cycle numbers up to about $3 \text{ cm}^{-1} \text{ MHz}^{-1}$ at 3500 flight cycles. The rate of aging of the thermoplastic indicates that the low strain protocol causes the thermoplastic's slope of attenuation to increase as $6 \times 10^{-4} \text{ cm}^{-1} \text{ MHz}^{-1}$ per flight cycle. The rate of aging of the thermoplastic for the high strain protocol causes the thermoplastic's β to increase as $10.8 \times 10^{-4} \text{ cm}^{-1} \text{ MHz}^{-1}$ per flight cycle. As was suggested earlier from the slope of attenuation images, a 50% increase in the strain causes the β attenuation to nearly double for the thermoplastics according to figure 4.

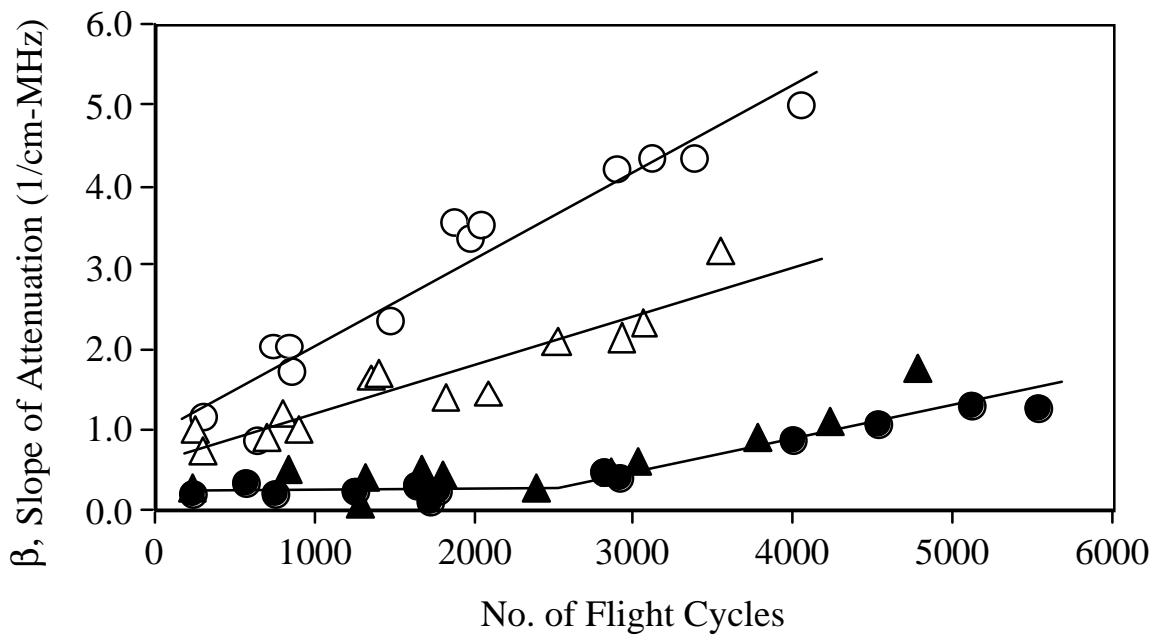


Figure 4. Graph of slope of attenuation vs. number of flight cycles. The open triangles (Δ) represent the thermoplastic samples, low strain protocol. The open circles (\bigcirc) represent the thermoplastic samples, high strain protocol. The solid triangles (\blacktriangle) are the thermoset samples, low strain protocol and the solid circles (\bullet) are thermoset samples, high strain protocol. The lines are least square fit trend lines for the thermoplastic high strain and low strain data groups and for the thermosets' low flight cycle numbers and high flight cycle numbers data groups.

The inclusion of thermoset composite data in figure 4 helps to show the relative ranges of the slope of attenuation for a thermoplastic in comparison to a thermoset. In addition it illustrates the different behavior of the two materials to thermal and fatigue loads. The thermoset has a strikingly different behavior. The thermoset composite indicates little dependence upon the relative load levels used. Also, very noticeable is the behavior in the rate of change of the aging of the thermoset. Little change is noted in the thermoset composite's slope of attenuation value up to about 2500 flight cycles. After that time, there is an obvious rise in the slope of attenuation where the values of slope of attenuation increases from less than $0.5 \text{ cm}^{-1} \text{ MHz}^{-1}$ at 2500 flight cycles up to about $1.5 \text{ cm}^{-1} \text{ MHz}^{-1}$ at 5500 flight cycles. The monotonic rate dependence of β for the thermoplastic suggests that possibly only one aging mechanism is dominant, such as microcracking of the matrix. This is in contrast to the thermoset whose more complex dependence on number of flight cycles suggests a more complex interaction is occurring such as additional curing with thermal cycling at low flight cycles with the juxtaposition of microcracking. The rate of microcrack formation in these materials is a measurement that has not been completed at this time. The rate of change in the slope of attenuation per flight cycle for the thermoset composite was $0.15 \times 10^{-4} \text{ cm}^{-1} \text{ MHz}^{-1}$ per flight cycle at low flight cycle numbers. This rate appears to jump to $3.8 \times 10^{-4} \text{ cm}^{-1} \text{ MHz}^{-1}$ per flight cycle after about 2500 flight cycles.

Finally, Table I lists some preliminary destructive testing that has been done to date on these samples to elucidate the properties of these thermoplastic composites. The data being reported in Table I is for open hole compression and tension testing of thermoplastic samples that either underwent no flight cycles or approximately 1200 flight cycles. Table I shows that there is no discernable effect on the ultimate strength of these composites at this level of aging. Similar results were seen for various modulus measurements. From figure 4, the amount of change in the slope of attenuation is evident at this number of flight cycles. In general these destructive tests measure in-plane properties of the composites which are

Table I. Ultimate Stress for Open Hole Tension and Compression Testing of Thermoplastic Samples.

No. of Flight Cycles	Strain Level	Ultimate Stress Open Hole Tension (psi \pm s. d.)	Ultimate Stress Open Hole Compression (psi \pm s. d.)
0	--	$6.63 \times 10^4 \pm 0.28$	$- 4.47 \times 10^4 \pm 0.12$
1349	Low	$6.63 \times 10^4 \pm 0.28$	$- 4.27 \times 10^4 \pm 0.18$
1190	High	$6.63 \times 10^4 \pm 0.28$	$- 4.31 \times 10^4 \pm 0.08$

dominated by the fiber's integrity. The measurements of β are more likely to reflect out-of-plane directions that are more indicative of matrix conditions such as microcracking. Therefore, the microstructural changes that are occurring in thermoplastic composites at this level of aging are affecting β before such changes can affect the gross mechanical properties of these materials.

CONCLUSION

Measurements of the ultrasonic slope of attenuation of thermoplastic composites undergoing large numbers of flight cycles were measured. After as few as 300 flight cycles, samples showed localized areas of increased attenuation for the high strain protocol. After more than 4000 cycles of thermal-mechanical loading the thermoplastic samples showed significant increases in the attenuation data for both low and high strain testing. High strain level effects on thermoplastics were demonstrably greater than from low strain levels. The slope of attenuation increases approximately linearly with number of flight cycles in the thermoplastic composites. This behavior is distinctly different from thermoset composites that show little effects of aging until after 2500 flight cycles. Finally, attenuation measurements are indicating material changes long before mechanical testing is being affected.

REFERENCES

1. *Nondestructive Testing*, ASTM Standard E664-93, Vol. 03.03, Easton, MD, 1994), pp. 264-266.
2. D. J. Chinn, P. F. Durbin, G. H Thomas, and S. E. Groves, in *Review of Progress in QNDE*, Vol. 16, Eds. D. O. Thompson and D. E. Chimenti (Plenum, New York, 1997), pp 1893-1901.
3. S.M. Handley, M.S. Hughes, J.G. Miller, and E.I. Madaras, *Proc. IEEE Ultrasonics Symposium* (Denver, 1987), 87CH2492-7, pp. 827-830, 1988.
4. David K. Hsu and Ali Minachi, in *Review of Progress in QNDE*, Vol. 9B, Eds. D.O. Thompson and D.E. Chimenti, (Plenum, New York, 1990), pp. 1481-1488